archive ouverte UNIGE
http://archive-ouverte.unige.ch

Article

Psychotic symptoms influence the development of anterior cingulate BOLD variability in 22q11.2 deletion syndrome

ZOELLER, Daniela, *et al*.

Abstract

Chromosome 22q11.2 deletion syndrome (22q11DS) is a neurodevelopmental disorder associated with a broad phenotype of clinical, cognitive and psychiatric features. Due to the very high prevalence of schizophrenia (30-40%), the investigation of psychotic symptoms in the syndrome is promising to reveal biomarkers for the development of psychosis, also in the general population. Since schizophrenia is seen as a disorder of the dynamic interactions between brain networks, we here investigated brain dynamics, assessed by the variability of blood oxygenation level dependent (BOLD) signals, in patients with psychotic symptoms. We included 28 patients with 22q11DS presenting higher positive psychotic symptoms, 29 patients with lower positive psychotic symptoms and 69 healthy controls between 10 and 30years old. To overcome limitations of mass-univariate approaches, we employed multivariate analysis, namely partial least squares correlation, combined with proper statistical testing, to analyze resting-state BOLD signal variability and its age-relationship in patients with positive psychotic symptoms. Our results revealed a missing [...]

Reference

ZOELLER, Daniela, *et al*. Psychotic symptoms influence the development of anterior cingulate BOLD variability in 22q11.2 deletion syndrome. *Schizophrenia Research*, 2018, vol. 193, p. 319-328

PMID : 28803847
DOI : 10.1016/j.schres.2017.08.003

Available at:
http://archive-ouverte.unige.ch/unige:97033

Disclaimer: layout of this document may differ from the published version.

UNIVERSITÉ DE GENÈVE

Psychotic symptoms influence the development of anterior cingulate BOLD variability in 22q11.2 deletion syndrome.

Daniela Zöller[a,b,c], Maria Carmela Padula[c], Corrado Sandini[c], Maude Schneider[c], Elisa Scariati[c], Dimitri Van De Ville[a,b], Marie Schaer[c], Stephan Eliez[c]

[a] *Medical Image Processing Laboratory, Institute of Bioengineering, École Polytechnique Fédérale de Lausanne (EPFL), Lausanne, Switzerland*
[b] *Department of Radiology and Medical Informatics, University of Geneva, Geneva, Switzerland*
[c] *Developmental Imaging an Psychopathology Laboratory, Office Médico-Pédagogique, Department of Psychiatry, University of Geneva, Geneva, Switzerland*

Abstract

Chromosome 22q11.2 deletion syndrome (22q11DS) is a neurodevelopmental disorder associated with a broad phenotype of clinical, cognitive and psychiatric features. Due to the very high prevalence of schizophrenia (30-40 %), the investigation of psychotic symptoms in the syndrome is promising to reveal biomarkers for the development of psychosis, also in the general population. Since schizophrenia is seen as a disorder of the dynamic interactions between brain networks, we here investigated brain dynamics, assessed by the variability of blood oxygenation level dependent (BOLD) signals, in patients with psychotic symptoms. We included 28 patients with 22q11DS presenting higher positive psychotic symptoms, 29 patients with lower positive psychotic symptoms and 69 healthy controls between 10 and 30 years old. To overcome limitations of mass-univariate approaches, we employed multivariate analysis, namely partial least squares correlation, combined with proper statistical testing, to analyze resting-state BOLD signal variability and its age-relationship in patients with positive psychotic symptoms. Our results revealed a missing positive age-relationship in the dorsal anterior cingulate cortex (dACC) in patients with higher positive psychotic symptoms, leading to globally lower variability in the dACC in those patients. Patients without positive psychotic symptoms and healthy controls had the same developmental trajectory in this region. Alterations of brain structure and function in the ACC have been previously reported in 22q11DS and linked to psychotic symptoms. The present results support the implication of this region in the development of psychotic symptoms and suggest aberrant BOLD signal variability development as a potential biomarker for psychosis.

Keywords: BOLD signal variability, psychotic symptoms, 22q11.2 deletion syndrome, salience network

1. Introduction

Chromosome 22q11.2 deletion syndrome (22q11DS) is a neurodevelopmental disorder that comes with a vast cognitive and clinical phenotype (Oskarsdóttir et al., 2004; Maeder et al., 2016; Karayiorgou et al., 2010; McDonald-McGinn et al., 2015). The prevalence of schizophrenia in adult patients with the disorder is estimated at 30 % to 40 % (Murphy et al., 1999; Lewandowski et al., 2007; Schneider et al., 2014), which makes the deletion syndrome a model for the study of neurodevelopmental markers of psychosis and schizophrenia (Bassett & Chow, 1999).

Even though the exact neural mechanisms that may underlay the pathophysiology of psychosis and schizophrenia remain uncertain, schizophrenia is commonly seen as a disorder of functional network dysconnectivity rather than regionally specific pathophysiology (Friston et al., 1996; Friston, 1998). The recently proposed triple network model (Menon, 2011) sees mental disorders as a disruption of the interaction between three large scale brain networks in particular, namely the default mode network (DMN), the central executive network (CEN) and the salience network (SN). Findings in schizophrenia confirm and emphasize this hypothesis as a model for the disorder (Nekovarova et al., 2014). More precisely, structural and functional findings in the anterior cingulate cortex and the insula, two main regions of the SN (Nekovarova et al., 2014), suggest that disruptions in the SN mediate the altered relationship between DMN and CEN.

Since alterations in schizophrenia are obviously complex and more and more research confirms the impairment of brain dynamics in the disorder (Van Den Heuvel & Fornito, 2014), the investigation of brain dynamics in psychosis seems a promising approach when searching for neural correlates of its development. One simple approach to probe into dynamic brain function is moment-to-moment blood oxygenation level dependent (BOLD) signal variability (Garrett et al., 2013b). Even though it is not com-

*Corresponding author
Email address: daniela.zoller@epfl.ch (Daniela Zöller)

monly considered in resting-state functional magnetic resonance imaging (fMRI) studies, its implication in development and cognitive performance suggests its importance for healthy brain function (Grady & Garrett, 2014). Indeed, higher temporal signal variability reflects a higher dynamic range and network complexity, which is crucial for the function of neural systems (Deco et al., 2009, 2011; Garrett et al., 2013b; McIntosh et al., 2010). Findings in electroencephalography (EEG), magnetoencephalography (MEG) and fMRI suggest that brain variability increases from child- to adulthood (McIntosh et al., 2008; Lippé et al., 2009; Misić et al., 2010; Miskovic et al., 2016; Zöller et al., 2017) and is reduced under anesthesia (Huang et al., 2016). Furthermore higher variability has been linked to better cognitive performance (Garrett et al., 2013a, 2014), cognitive flexibility (Armbruster-Genc et al., 2016) and better pain coping (Rogachov et al., 2016).

While there are several studies relating psychosis in 22q11DS to altered brain morphology and structural connectivity (Scariati et al., 2016a), only few investigated brain function in relationship to psychosis (Debbané et al., 2012; Mattiaccio et al., 2016; Scariati et al., 2014; Padula et al., 2017; Tomescu et al., 2014). Two resting-state fMRI studies on whole brain functional connectivity linked increased DMN activity in 22q11DS to psychotic symptoms (Debbané et al., 2012; Mattiaccio et al., 2016). Padula et al., 2017 investigated functional connectivity within and between DMN, CEN and SN in 22q11DS, but did not find any significant relationship with psychotic symptoms. Using a multivariate approach, another resting-state fMRI study revealed a connectivity pattern that discriminated patients presenting prodromal positive symptoms (Scariati et al., 2014). The pattern included the anterior cingulate, right inferior frontal and left superior temporal cortices. Furthermore, an EEG study in patients with 22q11DS has linked altered SN function (i.e. the over-representation of EEG microstate C) to the presence of hallucinations (Tomescu et al., 2014; Britz et al., 2010).

While we already investigated BOLD signal variability alterations and development in 22q11DS (Zöller et al., 2017), to date no study has revealed its relationship to psychotic symptoms in 22q11DS. Here, we employed partial least squares correlation (PLSC; Krishnan et al., 2011) as a powerful multivariate approach to reveal alterations and age-relationship of BOLD variability related to psychotic symptoms in 22q11DS. We furthermore compared BOLD variability in patients with and without psychotic symptoms to healthy controls (HCs) to evaluate alterations intrinsic to the presence of psychotic symptoms.

2. Methods

2.1. Participants

In the present study, we included 57 patients with 22q11DS aged between 10 and 30 years and 69 HCs in the same age range. HCs were recruited amongst siblings of the patients and through the Geneva state school system. Within the group of patients with the microdeletion, psychotic symptoms were assessed using the Structured Interview of Prodromal Symptoms (SIPS; Miller et al., 1995). Patients with a score of >= 3 in at least one of the positive SIPS sub-scales (i.e. Unusual Thought Content, Suspiciousness, Grandiosity, Hallucinations, and Disorganised Communication) were considered as having attenuated positive symptoms aside the criteria of frequency and duration (Fusar-Poli et al., 2013). Amongst the patients with 22q11DS, 28 patients were diagnosed with at least attenuated positive symptoms (PS+), while the remaining 29 had low positive symptoms scores (<= 2) and were included in the PS- group. In the PS+ group, five patients were diagnosed with a psychotic disorder according to DSM-IV-TR criteria (see Supplementary Table S1). For more detailed demographic information, see table 1. Written informed consent was received from participants and their parents (for subjects younger than 18 years old). The research protocols were approved by the Institutional Review Board of Geneva University School of Medicine. For a summary on criteria for the exclusion of subjects from our initial cohort and information on subjects included in our previous fMRI studies refer to Supplementary Materials.

2.2. Image acquisition

All MRI brain scans were acquired at the Centre d'Imagerie BioMédicale (CIBM) in Geneva on a Siemens Trio (N = 86: 53 HCs, 18 PS+, 15 PS-) and a Siemens Prisma (N = 40: 16 HCs, 10 PS+, 14 PS-) 3 Tesla scanner. Structural images were obtained with a T1-weighted sequence of $0.86\times0.86\times1.1\,\mathrm{mm}^3$ volumetric resolution (192 slices, TR = 2500 ms, TE = 3 ms, acquisition matrix = 224 × 256, field of view = $22\,\mathrm{cm}^2$, flip angle = 8°). Resting-state fMRI data were recorded with a T2-weighted sequence of 8 minutes (voxel size = $1.84\times1.84\times3.2$ mm, 38 slices, TR = 2400 ms, TE = 30 ms, flip angle = 85°). During the resting-state session, participants were instructed to let their minds wander and not to think of anything in particular, while fixing a cross on the screen, and not to fall asleep.

2.3. Preprocessing

In the present study, data were processed similarly as in our previous paper on BOLD variability in 22q11DS (Zöller et al., 2017). MRI preprocessing was done using Statistical Parametric Mapping (SPM12, Wellcome Trust Centre for Neuroimaging, London, UK: http://www.fil.ion.ucl.ac.uk/spm/) and functions of the Data Processing Assistant for Resting-State fMRI (DPARSF; Yan, 2010) and Individual Brain Atlases using Statistical Parametric Mapping (IBASPM; Aleman-Gomez et al., 2006) toolboxes. After realignment of functional scans, we applied spatial smoothing with an isotropic Gaussian kernel of 6 mm full width half maximum (FWHM) and coregistered structural scans to the

Table 1: Demographic information.

	PS+	**PS-**	**HC**	**p-value PS+ vs. PS-**	**p-value PS+ vs. HC**	**p-value PS- vs. HC**
Number of subjects (M/F)	28 (12/16)	29 (14/15)	69 (30/39)	0.6813	0.9554	0.6629
Age mean±SD	17.93±4.50	17.44±4.54	17.60±5.22	0.6846	0.7651	0.8918
(range)	(10.3-27.9)	(11.1-28.4)	(10.0-29.6)			
Right handed*	60.71 %	96.55%	78.79 %	<0.001	0.0697	0.0288
IQ**	67.25±9.82	70.21±13.71	108.86±13.47	0.3563	<0.001	<0.001
N. subjects meeting criteria for psychiatric diagnosis* **	**20**	**14**	**N/A**			
Anxiety disorder	5	4	N/A			
Attention deficit	1	1	N/A			
hyperactivity disorder			N/A			
Mood disorder	2	3	N/A			
Schizophrenia spectrum disorders	2	0	N/A			
More than one	10	6	N/A			
psychiatric disorder						
N. subjects medicated						
Methylphenidate	1	7	0			
Antipsychotics	3	0	0			
Anticonvulsants	1	0	0			
Antidepressants	3	1	0			
More than one	2	0	0			
class of medication						

* Handedness was measured using the Edinburgh laterality quotient, right handedness was defined by a score of more than 50. ** IQ was measured using the Wechsler Intelligence Scale for Children–III (Wechsler, 1991) for children and the Wechsler Adult Intelligence Scale–III (Wechsler, 1997) for adults. *** The presence of psychiatric disorders was evalutated during a clinical interview with the patients using the Diagnostic Interview for Children and Adolescents Revised (DICA-R; Reich, 2000), the psychosis supplement from the Kiddie-Schedule for Affective Disorders and Schizophrenia Present and Lifetime version (K-SADS-PL; Kaufman et al., 1997) and the Structured Clinical Interview for DSM-IV Axis I Disorders (SCID-I; First et al., 1996).

functional mean. Structural images were segmented with the SPM12 *Segmentation* algorithm (Ashburner & Friston, 2005) and a study-specific template was generated using Diffeomorphic Anatomical Registration using Exponential Lie algebra (DARTEL; Ashburner, 2007). Then, the first five functional scans were excluded from the analysis, mean white-matter and CSF signals were regressed from the BOLD time series, which were then filtered with a bandwidth of 0.01 Hz to 0.1 Hz. For a more extended correction of motion artifacts, we further applied motion scrubbing (Power et al., 2012), excluding frames with a framewise displacement of more than 0.5 mm, as well as one frame before and two frames after. Refer to Supplementary Table S2 for a summary on motion characteristics of the groups before and after motion scrubbing.

2.4. BOLD signal variability

At every voxel, BOLD signal variability was defined as the standard deviation of preprocessed time series (SD_{BOLD}) in subject space. Afterwards, every subject's SD_{BOLD} map was spatially normalized to the study-specific DARTEL template. Spatial normalization was applied after SD_{BOLD} computation, as in this way voxel-wise variability measures such as ALFF are less affected by spatial distortions (Wu et al., 2011). Then, SD_{BOLD} maps were thresholded in order to keep only voxels with a probability higher than 0.2 of laying inside the gray matter and spatially z-scored for every subject.

2.5. Partial least squares correlation

We employed PLSC (Krishnan et al., 2011; McIntosh & Lobaugh, 2004) to investigate multivariate alterations and age-relationship of SD_{BOLD} related to the diagnosis. Figure 1 shows a schematic representation of the steps for PLSC.

By extracting principal components of covariance between brain data and a set of subject-specific design variables (here: diagnosis, age and their interaction), PLSC uncovers brain patterns with the strongest multivariate correlation to the design variables. We first computed the partial correlation matrix across subjects $\mathbf{R}$ between SD_{BOLD} data $\mathbf{X}$ and design variables $\mathbf{Y}$. Brain and design data were z-scored across subjects before applying PLSC, and motion (i.e. average framewise displacement), scanner type (Trio or Prisma) and full-scale IQ were included as nuisance regressors. Then, so called latent variables were extracted by singular value decomposition (SVD) of $\mathbf{R} = \mathbf{USV}^{\mathrm{T}}$. In this work, we refer to the latent variables as "correlation components". Each of the components is associated with a singular value (diagonal elements of $\mathbf{S}$) indicating how much of the correlation is explained by this component. Design saliences in $\mathbf{U}$ contain the design loadings for every component that indicate how strong each of the design variables contributes to the brain-design correlation explained by this component. Brain saliences in $\mathbf{V}$ contain a brain pattern for every component, representing how strong every voxel contributes to the brain-design

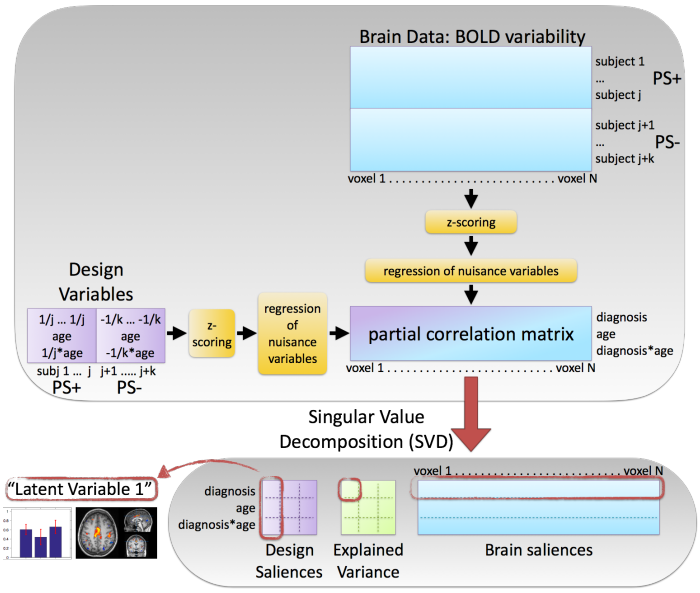

Figure 1: Schematic representation of PLSC.

correlation explained by this component. Furthermore, so-called "brain-scores" were obtained for every subject by projecting the subject's SD_{BOLD} map (in $\mathbf{X}$) on the brain salience pattern (in $\mathbf{V}$) of the correlation components: $\mathbf{L_X} = \mathbf{XV}$. So-called "design scores" were computed similarly: $\mathbf{L_Y} = \mathbf{YU}$.

In order to evaluate how many components explain a significant amount of the correlation, we employed permutation testing. By shuffling the elements of $\mathbf{Y}$ 1000 times while keeping the order of $\mathbf{X}$ unchanged, we determined the null distribution of explained correlation. A component was considered significant (p=0.05) if its singular value was higher than 95 % of its null distribution. For the significant components, we furthermore evaluated the robustness of brain and design saliences using a bootstrapping procedure with 500 random samples with replacement. For every bootstrap sample, we recalculated design and brain saliences ($\mathbf{U}$ and $\mathbf{V}$) and so obtained a typical bootstrap distribution of the salience values. Brain bootstrap ratios, calculated by dividing brain salience values by their standard deviations, indicate for every voxel its contribution to the brain-design correlation and can be interpreted similarly to z-scores (Krishnan et al., 2011).

3. Results

3.1. Different age-relationship in PS+ and PS- patients

Our main goal was to investigate alterations and age-relationship of SD_{BOLD} related to the presence of psychotic symptoms in patients with 22q11DS. We used PLSC with the design variables diagnosis (1 for PS+ patients, -1 for PS- patients), age and their interaction. Motion, scanner type and full-scale IQ were included as nuisance regressors. PLSC resulted in two significant correlation components.

Figure 2 shows the design and brain saliences for the first significant correlation component (p=0.002) resulting from PLSC comparing the PS+ and PS- groups. This first component represents a brain pattern where SD_{BOLD} is strongly correlated with age in PS- patients. This age-relationship, however, is not evident in the PS+ group and the average SD_{BOLD} in the pattern is lower in the PS+ group. The largest cluster of the corresponding pattern (see also Supplementary Table S3) is located in the dorsal anterior cingulate (dACC). Positive brain salience values indicate that SD_{BOLD} in PS- patients is increasing over age in this area and is globally higher in PS- patients than in PS+ patients.

Figure 3 shows design and brain salience of the second significant correlation component (p=0.014) of the comparison of PS+ and PS- patients. This component represents a brain pattern where SD_{BOLD} is correlated with age in the PS+ group, whereas PS- patients show an opposed relationship with age. The corresponding pattern (see also Supplementary Table S4) contains bilateral negative clusters spanning the prefrontal and orbitofrontal cortices, indicating that there, SD_{BOLD} decreases with age in PS+ patients and increases with age in PS- patients. It furthermore includes positive clusters in occipital, secondary visual regions, indicating an increase over age of SD_{BOLD} in PS+ patients, while SD_{BOLD} in PS- patients is decreasing.

3.2. Comparison of PS+ patients, PS- patients and HCs

In order to compare SD_{BOLD} in the two 22q11DS subgroups against HCs, we employed a second PLSC, this time with five design variables: the diagnosis of 22q11DS (diagnosis 1: 1 for PS+ and PS- patients, -1 for HCs); the presence of psychotic symptoms (diagnosis 2: 1 for PS+ patients, -1 for PS- patients, and 0 for HCs); age; the interaction between age and diagnosis 1, and the interaction between age and diagnosis 2. Motion and scanner type were included as nuisance regressors. IQ was not included to avoid the insensitivity to SD_{BOLD} group differences introduced by systematic group differences in full-scale IQ. Again, PLSC resulted in two significant correlation components.

Figure 4 shows design and brain saliences for the first significant correlation component (p<0.0001) resulting from the comparison of patients with 22q11DS (PS+ and PS-) to HCs. The corresponding pattern shows areas where SD_{BOLD} in patients with 22q11DS is different from HCs, but where patients within the 22q11DS group do not show significant differences. The corresponding brain salience pattern (see also Supplementary Table S5) includes numerous areas distributed over the whole brain. SD_{BOLD} in cortical regions, including the CEN and parts of the DMN, is mainly reduced in 22q11DS, whereas in subcortical regions such as caudate and thalamus, SD_{BOLD} is higher in 22q11DS. Interestingly, dACC is not part of this pattern, which suggests that alterations in dACC (see section 3.1), specifically differentiate patients with 22q11DS with higher symptoms.

Figure 5 shows design and brain saliences for the second significant correlation component (p=0.001). This component contains a pattern where SD_{BOLD} is correlated with age in HCs and in patients without psychotic symptoms (PS-). Patients with psychotic symptoms (PS+), however, do not show any correlation with age inside this pattern. Besides the superior motor area, caudate and amygdala, the brain pattern also includes the dACC (see also Supplementary Table S6). An increase of SD_{BOLD} over age in these regions is thus common to PS- patients and HCs, but absent in PS+ patients.

3.3. Stability of the results

Exclusion of the five patients diagnosed with a psychotic disorder (see section 2.1 and Supplementary Table S1) did not alter the present results besides slightly higher p-values, caused by the lower statistical power. Due to this increase, component 2 in the first analysis (see figure 3) was not significant anymore (p>0.05), but all other results remained significant with similar brain and design saliences.

Inclusion or exclusion of scanner type as covariate did not significantly alter the results.

Motion is a major concern in the analysis of BOLD variability. Supplementary Section S3 outlines the correlations of the resulting brain scores with motion. There were no significant motion effects in the first analysis, and only low motion effects in brain scores of healthy controls in the second analysis.

4. Discussion

The central finding of the present study was that BOLD variability (SD_{BOLD}) in the dACC is lower in patients with higher positive psychotic symptoms than in patients with lower symptoms (section 3.1). We found evidence that BOLD variability in the dACC does not change over age in PS+ patients, but increases with age in PS- patients and HCs (sections 3.1 and 3.2). Furthermore, dACC was not part of a pattern where BOLD variability was altered in patients with 22q11DS compared to HCs, independent of the presence of psychotic symptoms (section 3.2), indicating that alterations in dACC are intrinsic to the presence of higher psychotic symptoms in 22q11DS. Additionally, we found evidence for a pattern where only patients with psychotic symptoms show a significant relationship of BOLD variability with age (section 3.1).

In the following, we will discuss the relevance of alterations found in the dACC related to psychotic symptoms in 22q11DS and in the general population. We furthermore will comment on the age-relationship of BOLD variability that was evident only in PS+ patients, as well as on the BOLD variability alterations in both 22q11DS subgroups.

Our observation of altered BOLD variability in the dACC is in line with several previous findings in 22q11DS

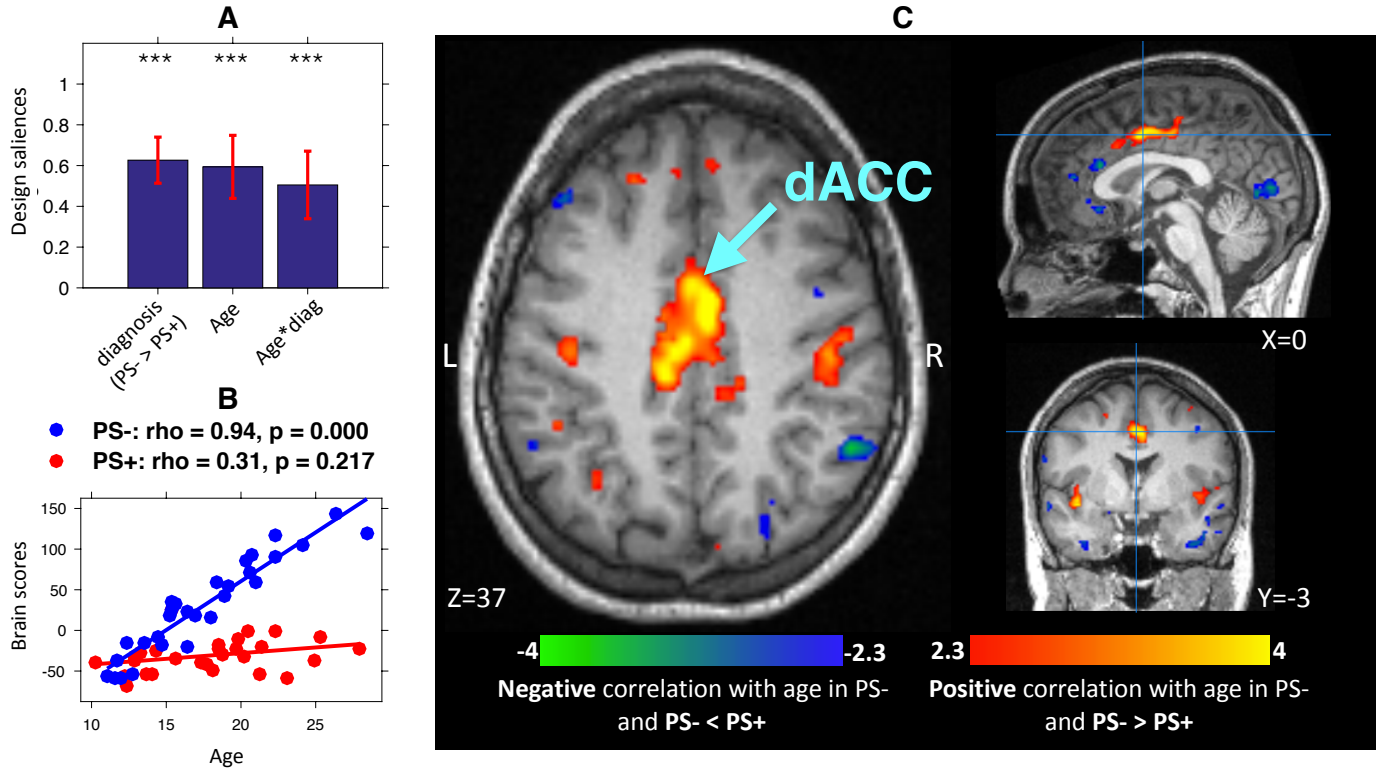

Figure 2: First significant correlation component (p=0.002) resulting from PLSC comparing PS+ patients to PS- patients. Subfigures show design saliences with bootstrap error bars (A), brain scores as a function of age (B), and brain salience bootstrap ratios (C). The component reveals that PS- patients have increasing SD_{BOLD} in the dACC, while in PS+ patients this age-relationship is absent. dACC - dorsal anterior cingulate cortex; ** p<0.01; *** p<0.001.

and schizophrenia. In fact, alterations in the ACC have been reported in 22q11DS (Scariati et al., 2016a; Schneider et al., 2012; Rihs et al., 2013; Schaer et al., 2010) and linked to the presence of psychotic symptoms within the syndrome using diverse modalities (Dufour et al., 2008; Scariati et al., 2014; Kates et al., 2015; Ottet et al., 2013; Tomescu et al., 2014). Structural MRI studies have reported grey matter volume reductions in 22q11DS which are most pronounced in the ACC (Schaer et al., 2010) and linked to the presence of psychotic symptoms in 22q11DS (Dufour et al., 2008). Furthermore, white matter dysconnectivity in cortical midline structures including the ACC has been related to psychotic symptoms in patients with the microdeletion (Kates et al., 2015; Ottet et al., 2013; reviewed in Scariati et al., 2016a). In a recent study conducted by our group, also structural connectivity measured by structural covariance, was found to be altered in the ACC and medial prefrontal cortex of patients with 22q11DS with psychotic symptoms (Sandini et al., 2017). Functional MRI studies in 22q11DS reported reduced resting-state functional connectivity in the ACC of patients with prodromal symptoms (Scariati et al., 2014), as well as functional hypo-activation in ACC during a self-referential task, which was correlated with the severity of positive symptoms (Schneider et al., 2012). Finally, recent EEG studies revealed a microstate C over-representation that was correlated with the presence of hallucinations in 22q11DS (Tomescu et al., 2014, 2015). This EEG microstate C has been related to fMRI activity in the ACC (Britz et al., 2010).

Also in the general population, changes of brain structure and function is the ACC have repeatedly been reported in subjects at ultra high risk for psychosis and in schizophrenia (Fornito et al., 2008, 2009; Reid et al., 2010; Jung et al., 2010; Pettersson-Yeo et al., 2011; Lord et al., 2011; Allen et al., 2010; Nekovarova et al., 2014). Alterations in the ACC have been linked to self-monitoring deficits (Allen et al., 2008) and auditory-verbal hallucinations (Allen et al., 2007).

The dACC is an area implicated in goal-directed behavior, self-related processing, and cognitive control (Shenhav et al., 2013; Sridharan et al., 2008; Uddin, 2015). It is a central hub of the SN (Menon & Uddin, 2010). Our observation of increasing BOLD variability in the SN of PS- patients and healthy controls is in line with a recent study, also showing linearly increasing resting-state BOLD variability in SN nodes(Nomi et al., 2017). Lower BOLD variability in the PS+ group may reflect a dysfunction in the attribution of salience. Such aberrant salience attribution has been suggested as mechanism for the development of

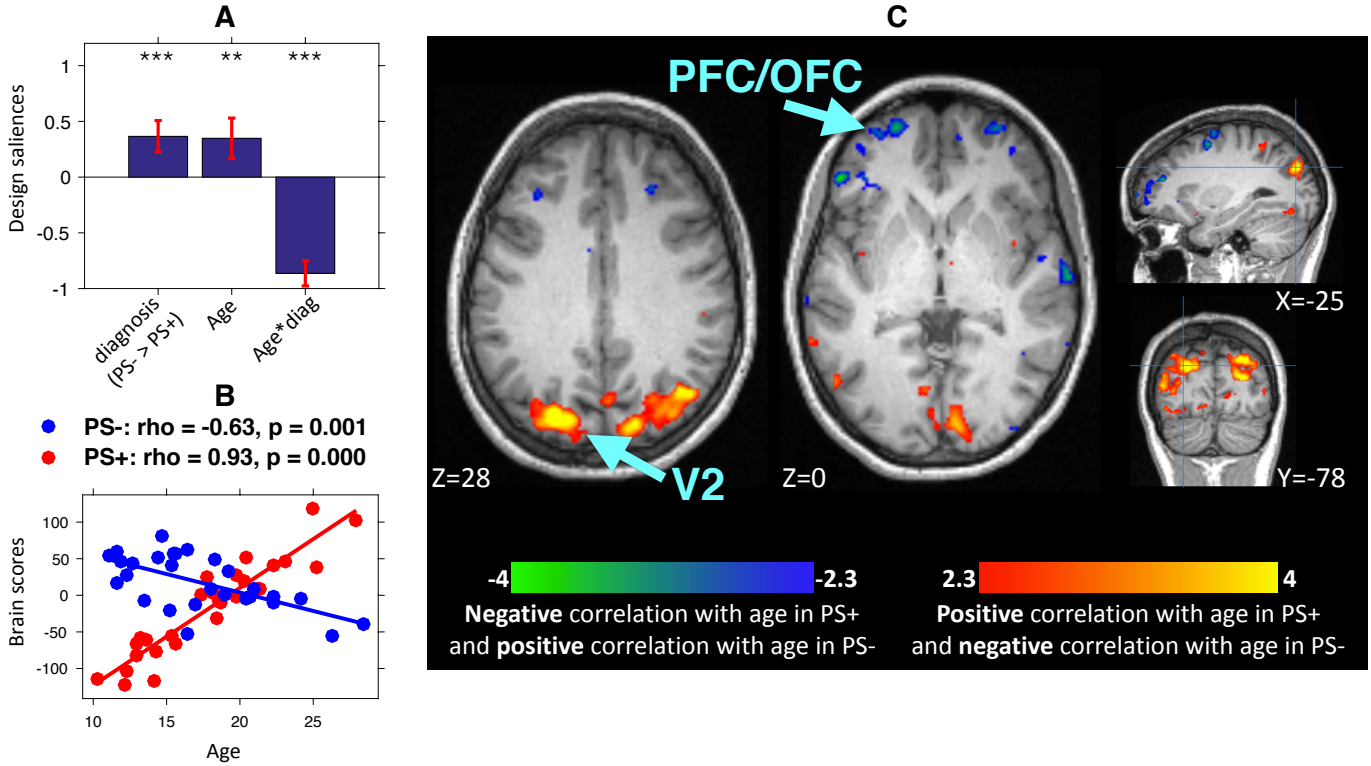

Figure 3: Second significant correlation component (p=0.014) resulting from PLSC comparing PS+ patients to PS- patients. Subfigures show design saliences with bootstrap error bars (A), brain scores as a function of age (B), and brain salience bootstrap ratios (C). The component uncovers that in PS+ patients, SD_{BOLD} decreases over age in the PFC/OFC and increases over age in V2. In PS- patients, SD_{BOLD} in this pattern has an opposed relationship with age: increasing in the PFC/OFC and decreasing in V2. OFC - orbitofrontal cortex; PFC - prefrontal cortex; V2 - secondary visual cortex; *** p<0.001.

psychosis and schizophrenia (Kapur, 2003). Higher BOLD variability has been suggested to reflect optimal shifting between integrative and segregative brain states (Nomi et al., 2017; Tognoli & Kelso, 2014). Speculatively, lower BOLD variability in the dACC may thus disrupt the shifting ability of the SN, leading to a disability to correctly treat salience of external and internal stimuli.

Beyond the BOLD variability reduction in the dACC, we found that patients with psychotic symptoms have a pattern of aberrant age-relationship with increasing BOLD variability in visual regions and decreasing BOLD variability in the prefrontal and orbitofrontal coritces. Structural and functional alterations in frontal regions have been reported in psychosis and schizophrenia, including volume reductions (Jung et al., 2010), structural and functional dysconnectivity (Pettersson-Yeo et al., 2011), and increased brain signal variability (Hoptman et al., 2010; Takahashi et al., 2010). Also structural and functional alterations in the visual cortex have been observed in schizophrenia (Narr et al., 2005; Yu et al., 2014; Butler et al., 2007), and may be related to deficits in visual processing (Butler et al., 2005). Together with the altered age-relationship in the dACC, these results suggest aberrant developmental trajectories related to psychotic symptoms and point towards aberrant BOLD variability development as a potential predictor for psychosis. As these results are limited by the cross-sectional nature of the analysis, this hypothesis should be confirmed in further studies including longitudinal data.

In our previous paper (Zöller et al., 2017), we compared BOLD variability in patients with 22q11DS to HCs without differentiating patients according to psychotic symptoms. Interestingly, we here observed a weaker correlation with age in 22q11DS than in HCs. In view of the present results, this difference can be explained by the absent age-relationship in patients with psychotic symptoms, while age-relationship of BOLD variability in patients without positive symptoms is as strong as in HCs.

5. Conclusions and Limitations

To our best knowledge, this is the first study investigating BOLD signal variability alterations related to psychosis in patients with 22q11DS. Firstly, we revealed reduced BOLD variability related to psychotic symptoms in the dACC, a region which is central for cognitive control and salience attribution and where alterations have been previously linked to psychotic symptoms in 22q11DS and the general population. In this region, patients without psychotic symptoms and HCs had similar levels of BOLD

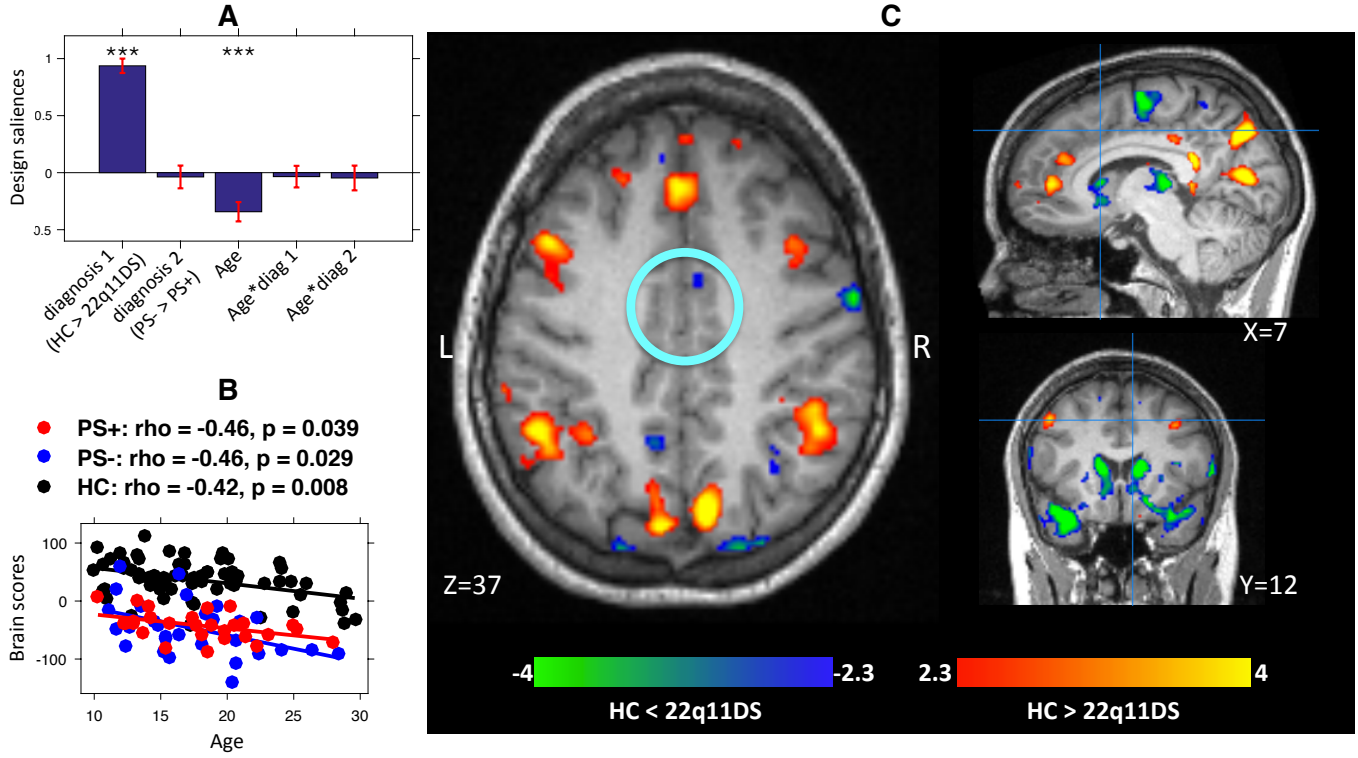

Figure 4: First significant correlation component (p<0.0001) resulting from PLSC comparing patients with 22q11DS to HCs. Subfigures show design saliences with bootstrap error bars (A), brain scores as a function of age (B), and brain salience bootstrap ratios (C). The component contains a pattern where SD_{BOLD} is higher (red) or lower (blue) in HCs compared to 22q11DS, with identical age-relationship in the three groups. The blue circle indicates the area in the dACC, where PS+ patients showed altered age-relationship compared to PS- patients (see section 3.1 and figure 2). This cluster is not different in 22q11DS compared to HCs. * p<0.05; ** p<0.01; *** p<0.001.

variability, suggesting that the reductions are intrinsic to the presence of psychotic symptoms. We furthermore retrieved a pattern of age-relationship specific to patients with psychotic symptoms, including frontal and occipital regions.

A main limitation of this study is the limited sample size over a relatively large age range. Furthermore, the cross-sectional nature of our data limits the interpretations to effects across subjects. Our results will need to be replicated in a larger sample and including longitudinal data to allow to conclude on true developmental effects.

Another confound might have been the heterogeneity in terms of symptoms severity and outcome of PS+ and PS- patients. Even though patients with positive psychotic symptoms are at higher risk to transition into psychosis, they may as well remain stable or even recover (Schneider et al., 2016; Schultze-Lutter et al., 2015; Fusar-Poli et al., 2012). In our sample, all those patients were included in the PS+ group. Also, since there was no follow-up yet for most of the younger subjects included in the PS- group, we cannot exclude that some of those subjects might, indeed, develop symptoms at an older age. In our results, the decrease in BOLD variability in patients with psychotic symptoms only becomes evident at an age above 15, while younger individuals with and without psychotic symptoms have similar values. This effect might be driven by the aforementioned limitation in the group assignment of young subjects. Other confounds that might have driven these results are the duration of the presence of symptoms, or effects of medication.

A possible confound regarding the analysis of SD_{BOLD} may have been differences in gray matter volume between the groups. Indeed, gray matter volume is known to be globally reduced in 22q11DS (Tan et al., 2009; Gothelf et al., 2008). However, as gray matter volume in the entire cortex decreases over development (Giedd et al., 1999; Gogtay et al., 2004), including it as a confounding variable would lead to insensitivity in detecting age-dependence specific to SD_{BOLD}. Since additionally, gray matter volume and SD_{BOLD} development do not seem to be directly linked (Bray, 2017), we did not to include gray matter volume as nuisance regressor.

6. Role of funding source

This research was supported by the Swiss National Research Foundation (SNF) [grant numbers 32473B_121996 and 234730_144260 to S. Eliez]. It was also supported by the National Center of Competence in Research (NCCR) "SYNAPSY — The Synaptic Bases of Mental Diseases"

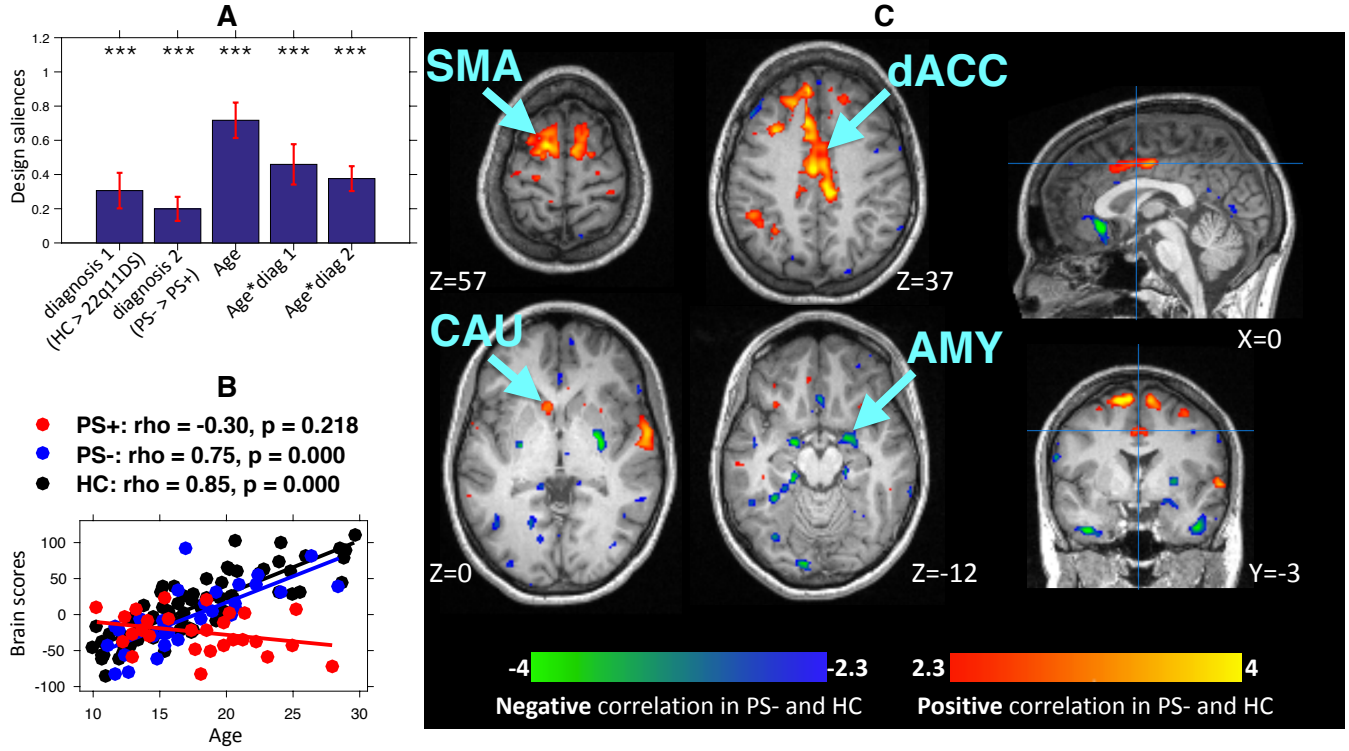

Figure 5: Second significant correlation component (p=0.001) resulting from PLSC comparing patients with 22q11DS to HCs. Subfigures show design saliences with bootstrap error bars (A), brain scores as a function of age (B), and brain salience bootstrap scores (C). The component contains a pattern where SD_{BOLD} is increasing (red) or decreasing (blue) in PS- patients and HCs, but where in PS+ patients do not show any significant relationship with age. Amongst other areas, the pattern includes the dACC. AMY - amygdala; CAU - caudate; dACC - dorsal anterior cingulate cortex; SMA - superior motor area; * p<0.05; *** p<0.001.

[SNF, grant numbers 51AU40_125759 and 51NF40_158776 to S. Eliez], as well as individual grants of the SNF to S. Eliez [grant number #145250] and M. Schaer [grant number #163859].

7. Contributors

Authors D.Z., M.C.P, M.Schaer and D.V.d.V. designed the study. Authors M.C.P., C.S., M.Schneider., M.Schaer. and S.E. collected the magnetic resonance imaging and clinical data. Authors D.Z. and D.V.d.V. designed and implemented the statistical analysis. Authors D.Z., M.C.P., C.S., E.S., M.Schneider, M.Schaer and S.E. contributed to the results interpretation, and author D.Z. wrote the first draft of the manuscript. All authors contributed to and have approved the final manuscript.

8. Conflict of Interest

All authors declare that they have no conflicts of interest.

9. Acknowledgements

We are grateful to the families who participated in our study and thank Sarah Menghetti and Léa Chambaz for their involvement with the families. We furthermore would like to acknowledge François Lazeyras and the group of CIBM for their support during data collection and Frédérique Bena Sloan for the genetic analysis.

References

Aleman-Gomez, Y., Melie-García, L., & Valdés-Hernandez, P. (2006). IBASPM: toolbox for automatic parcellation of brain structures. In *12th Annu. Meet. Organ. Hum. Brain Mapp.*.

Allen, P., Aleman, A., & McGuire, P. K. (2007). Inner speech models of auditory verbal hallucinations: evidence from behavioural and neuroimaging studies. *Int Rev Psychiatry*, *19*, 407–415. URL: `http://www.ncbi.nlm.nih.gov/pubmed/17671873`. doi:`10.1080/09540260701486498`.

Allen, P., Larøi, F., McGuire, P. K., & Aleman, A. (2008). The hallucinating brain: A review of structural and functional neuroimaging studies of hallucinations. *Neurosci. Biobehav. Rev.*, *32*, 175–191. doi:`10.1016/j.neubiorev.2007.07.012`.

Allen, P., Stephan, K. E., Mechelli, A., Day, F., Ward, N., Dalton, J., Williams, S. C., & McGuire, P. (2010). Cingulate activity and fronto-temporal connectivity in people with prodromal signs of psychosis. *Neuroimage*, *49*, 947–955. URL: `http://dx.doi.org/10.1016/j.neuroimage.2009.08.038`. doi:`10.1016/j.neuroimage.2009.08.038`.

Armbruster-Genc, D. J. N., Ueltzhoffer, K., & Fiebach, C. J. (2016). Brain Signal Variability Differentially Affects Cognitive Flexibility and Cognitive Stability. *J. Neurosci.*, *36*, 3978–3987. URL: `http://www.jneurosci.org/cgi/doi/10.1523/JNEUROSCI.2517-14.2016`. doi:`10.1523/JNEUROSCI.2517-14.2016`.

Ashburner, J. (2007). A fast diffeomorphic image registration algorithm. *Neuroimage*, *38*, 95–113. doi:10.1016/j.neuroimage.2007.07.007.

Ashburner, J., & Friston, K. J. (2005). Unified segmentation. *Neuroimage*, *26*, 839–851. doi:10.1016/j.neuroimage.2005.02.018.

Bassett, A. S., & Chow, E. W. C. (1999). 22q11 deletion syndrome: A genetic subtype of schizophrenia. *Biol. Psychiatry*, *46*, 882–891. doi:10.1016/S0006-3223(99)00114-6.

Bray, S. (2017). Age-associated patterns in gray matter volume, cerebral perfusion and BOLD oscillations in children and adolescents. *Hum. Brain Mapp.*, *00*. URL: http://doi.wiley.com/10.1002/hbm.23526. doi:10.1002/hbm.23526.

Britz, J., Van De Ville, D., & Michel, C. M. (2010). BOLD correlates of EEG topography reveal rapid resting-state network dynamics. *Neuroimage*, *52*, 1162–1170. doi:10.1016/j.neuroimage.2010.02.052.

Butler, P. D., Martinez, A., Foxe, J. J., Kim, D., Zemon, V., Silipo, G., Mahoney, J., Shpaner, M., Jalbrzikowski, M., & Javitt, D. C. (2007). Subcortical visual dysfunction in schizophrenia drives secondary cortical impairments. *Brain*, *130*, 417–430. doi:10.1093/brain/awl233.

Butler, P. D., Zemon, V., Schechter, I., Saperstein, A. M., Hoptman, M. J., Lim, K. O., Revheim, N., Silipo, G., & Javitt, D. C. (2005). Early-stage visual processing and cortical amplification deficits in schizophrenia. *Arch. Gen. Psychiatry*, *62*, 495–504. URL: http://eutils.ncbi.nlm.nih.gov/entrez/eutils/elink.fcgi?dbfrom=pubmed{&}id=15867102{&}retmode=ref{&}cmd=prlinks{%}5Cnfile:///Users/alexandershaw/Library/ApplicationSupport/Papers2/Articles/2005/Butler/ArchivesofGeneralPsychiatry2005Butler-3.pdf{%}5Cnpapers2:/. doi:10.1001/archpsyc.62.5.495.

Debbané, M., Lazouret, M., Lagioia, A., Schneider, M., Van De Ville, D., & Eliez, S. (2012). Resting-state networks in adolescents with 22q11.2 deletion syndrome: Associations with prodromal symptoms and executive functions. *Schizophr. Res.*, *139*, 33–39. URL: http://linkinghub.elsevier.com/retrieve/pii/S0920996412003143. doi:10.1016/j.schres.2012.05.021.

Deco, G., Jirsa, V. K., & McIntosh, A. R. (2011). Emerging concepts for the dynamical organization of resting-state activity in the brain. *Nat. Rev. Neurosci.*, *12*, 43–56. URL: http://dx.doi.org/10.1038/nrn2961. doi:10.1038/nrn2961.

Deco, G., Rolls, E. T., & Romo, R. (2009). Stochastic dynamics as a principle of brain function. *Prog. Neurobiol.*, *88*, 1–16. doi:10.1016/j.pneurobio.2009.01.006.

Dufour, F., Schaer, M., Debbané, M., Farhoumand, R., Glaser, B., & Eliez, S. (2008). Cingulate gyral reductions are related to low executive functioning and psychotic symptoms in 22q11.2 deletion syndrome. *Neuropsychologia*, *46*, 2986–2992. doi:10.1016/j.neuropsychologia.2008.06.012.

First, M., Gibbon, M., Spitzer, R., Williams, J., & Benjamin, L. (1996). Structured Clinical Interview for the DSM-IV Axis I Disorders (SCID-I). *Washington, DC Am. Psychiatr. Assoc.*, .

Fornito, A., Yücel, M., Dean, B., Wood, S. J., & Pantelis, C. (2009). Anatomical abnormalities of the anterior cingulate cortex in schizophrenia: Bridging the gap between neuroimaging and neuropathology. *Schizophr. Bull.*, *35*, 973–993. doi:10.1093/schbul/sbn025.

Fornito, A., Yung, A. R., Wood, S. J., Phillips, L. J., Nelson, B., Cotton, S., Velakoulis, D., McGorry, P. D., Pantelis, C., & Yücel, M. (2008). Anatomic Abnormalities of the Anterior Cingulate Cortex Before Psychosis Onset: An MRI Study of Ultra-High-Risk Individuals. *Biol. Psychiatry*, *64*, 758–765. doi:10.1016/j.biopsych.2008.05.032.

Friston, K. J. (1998). The disconnection hypothesis. *Schizophr. Res.*, *30*, 115–125. doi:10.1016/S0920-9964(97)00140-0.

Friston, K. J., Williams, S., Howard, R., Frackowiak, R. S., & Turner, R. (1996). Movement-related effects in fMRI time-series. *Magn. Reson. Med.*, *35*, 346–355. doi:DOI10.1002/mrm.1910350312.

Fusar-Poli, P., Bonoldi, I., Yung, A. R., Borgwardt, S., Kempton, M. J., Valmaggia, L., Barale, F., Caverzasi, E., & Mcguire, P. (2012). Predicting Psychosis. *Arch. Gen. Psychiatry*, *69*, 220–229. doi:10.1001/archgenpsychiatry.2011.1472.

Fusar-Poli, P., Borgwardt, S., Bechdolf, A., Addington, J., Riecher-Rössler, A., Schultze-Lutter, F., Keshavan, M., Wood, S., Ruhrmann, S., Seidman, L. J., Valmaggia, L., Cannon, T., Velthorst, E., De Haan, L., Cornblatt, B., Bonoldi, I., Birchwood, M., McGlashan, T., Carpenter, W., McGorry, P., Klosterkötter, J., McGuire, P., & Yung, A. (2013). The Psychosis High-Risk State. *JAMA Psychiatry*, *70*, 107. URL: http://archpsyc.jamanetwork.com/article.aspx?doi=10.1001/jamapsychiatry.2013.269. doi:10.1001/jamapsychiatry.2013.269.

Garrett, D. D., Kovacevic, N., McIntosh, A. R., & Grady, C. L. (2013a). The Modulation of BOLD Variability between Cognitive States Varies by Age and Processing Speed. *Cereb. Cortex*, *23*, 684–693. URL: http://www.cercor.oxfordjournals.org/cgi/doi/10.1093/cercor/bhs055. doi:10.1093/cercor/bhs055.

Garrett, D. D., McIntosh, A. R., & Grady, C. L. (2014). Brain Signal Variability is Parametrically Modifiable. *Cereb. Cortex*, *24*, 2931–2940. URL: http://www.cercor.oxfordjournals.org/cgi/doi/10.1093/cercor/bht150. doi:10.1093/cercor/bht150.

Garrett, D. D., Samanez-Larkin, G. R., MacDonald, S. W. S., Lindenberger, U., McIntosh, A. R., & Grady, C. L. (2013b). Moment-to-moment brain signal variability: A next frontier in human brain mapping? *Neurosci. Biobehav. Rev.*, *37*, 610–624. URL: http://dx.doi.org/10.1016/j.neubiorev.2013.02.015. doi:10.1016/j.neubiorev.2013.02.015. arXiv:NIHMS150003.

Giedd, J. N., Blumenthal, J., Jeffries, N. O., Castellanos, F. X., Liu, H., Zijdenbos, A., Paus, T., Evans, A. C., & Rapoport, J. L. (1999). Brain development during childhood and adolescence : A longitudinal MRI study. *Nat. Neurosci.*, (pp. 861–863). doi:10.1038/13158.

Gogtay, N., Giedd, J. N., Lusk, L., Hayashi, K. M., Greenstein, D., Vaituzis, A. C., Nugent III, T. F., Herman, D. H., Clasen, L. S., Toga, A. W., Rapoport, J. L., & Thompson, P. M. (2004). Dynamic mapping of human cortical development during childhood through early adulthood. *Proc.Natl.Acad.Sci.U.S.A*, *101*, 8174–8179. URL: file://c/Myfiles/RefMan10/RefManpdfs/16127.pdf.

Gothelf, D., Schaer, M., & Eliez, S. (2008). Genes, brain development and psychiatric phenotypes in velo-cardio-facial syndrome. *Dev. Disabil. Res. Rev.*, *14*, 59–68. doi:10.1002/ddrr.9.

Grady, C. L., & Garrett, D. D. (2014). Understanding variability in the BOLD signal and why it matters for aging. *Brain Imaging Behav.*, *8*, 274–283. URL: http://www.pubmedcentral.nih.gov/articlerender.fcgi?artid=3922711{&}tool=pmcentrez{&}rendertype=abstract. doi:10.1007/s11682-013-9253-0.

Hoptman, M. J., Zuo, X. N., Butler, P. D., Javitt, D. C., D'Angelo, D., Mauro, C. J., & Milham, M. P. (2010). Amplitude of low-frequency oscillations in schizophrenia: A resting state fMRI study. *Schizophr. Res.*, *117*, 13–20. URL: http://dx.doi.org/10.1016/j.schres.2009.09.030. doi:10.1016/j.schres.2009.09.030. arXiv:NIHMS150003.

Huang, Z., Zhang, J., Wu, J., Qin, P., Wu, X., Wang, Z., Dai, R., Li, Y., Liang, W., Mao, Y., Yang, Z., Zhang, J., Wolff, A., & Northoff, G. (2016). Decoupled temporal variability and signal synchronization of spontaneous brain activity in loss of consciousness: An fMRI study in anesthesia. *Neuroimage*, *124*, 693–703. URL: http://dx.doi.org/10.1016/j.neuroimage.2015.08.062. doi:10.1016/j.neuroimage.2015.08.062. arXiv:arXiv:1011.1669v3.

Jung, W. H., Jang, J. H., Byun, M. S., An, S. K., & Kwon, J. S. (2010). Structural brain alterations in individuals at ultra-high risk for psychosis: A review of magnetic resonance imaging studies and future directions. *J. Korean Med. Sci.*, *25*, 1700–1709. doi:10.3346/jkms.2010.25.12.1700.

Kapur, S. (2003). Psychosis as a state of aberrant salience: a framework linking biology, phenomenology, and pharmacology in schizophrenia. *Am. J. Psychiatry*, *160*, 13–23.

Karayiorgou, M., Simon, T. J., & Gogos, J. A. (2010). 22q11.2 microdeletions: linking DNA structural variation to brain dysfunction and schizophrenia. *Nat. Rev. Neurosci.*, *11*, 402–16. URL:

http://dx.doi.org/10.1038/nrn2841. doi:10.1038/nrn2841.

Kates, W. R., Olszewski, A. K., Gnirke, M. H., Kikinis, Z., Nelson, J., Antshel, K. M., Fremont, W., Radoeva, P. D., Middleton, F. A., Shenton, M. E., & Coman, I. L. (2015). White matter microstructural abnormalities of the cingulum bundle in youths with 22q11.2 deletion syndrome: Associations with medication, neuropsychological function, and prodromal symptoms of psychosis. *Schizophr. Res.*, *161*, 76–84. URL: http://dx.doi.org/10.1016/j.schres.2014.07.010. doi:10.1016/j.schres.2014.07.010.

Kaufman, J., Birmaher, B., Brent, D., Rao, U., Flynn, C., Moreci, P., Williamson, D., & Ryan, N. (1997). Schedule for Affective Disorders and Schizophrenia for School-Age Children-Present and Lifetime Version (K-SADS-PL): Initial Reliability and Validity Data. *J. Am. Acad. Child Adolesc. Psychiatry*, *36*, 980–988. URL: http://linkinghub.elsevier.com/retrieve/pii/S0890856709625557. doi:10.1097/00004583-199707000-00021.

Krishnan, A., Williams, L. J., McIntosh, A. R., & Abdi, H. (2011). Partial Least Squares (PLS) methods for neuroimaging: A tutorial and review. *Neuroimage*, *56*, 455–475. doi:10.1016/j.neuroimage.2010.07.034.

Lewandowski, K. E., Shashi, V., Berry, P. M., & Kwapil, T. R. (2007). Schizophrenic-like neurocognitive deficits in children and adolescents with 22q11 deletion syndrome. *Am. J. Med. Genet. Part B Neuropsychiatr. Genet.*, *144*, 27–36. doi:10.1002/ajmg.b.30379.

Lippé, S., Kovacevic, N., & McIntosh, A. R. (2009). Differential maturation of brain signal complexity in the human auditory and visual system. *Front. Hum. Neurosci.*, *3*, 48. doi:10.3389/neuro.09.048.2009.

Lord, L. D., Allen, P., Expert, P., Howes, O., Lambiotte, R., McGuire, P., Bose, S. K., Hyde, S., & Turkheimer, F. E. (2011). Characterization of the anterior cingulate's role in the at-risk mental state using graph theory. *Neuroimage*, *56*, 1531–1539. URL: http://dx.doi.org/10.1016/j.neuroimage.2011.02.012. doi:10.1016/j.neuroimage.2011.02.012.

Maeder, J., Schneider, M., Bostelmann, M., Debbané, M., Glaser, B., Menghetti, S., Schaer, M., & Eliez, S. (2016). Developmental trajectories of executive functions in 22q11.2 deletion syndrome. *J. Neurodev. Disord.*, *8*, 10. URL: http://www.jneurodevdisorders.com/content/8/1/10. doi:10.1186/s11689-016-9141-1.

Mattiaccio, L. M., Coman, I. L., Schreiner, M. J., Antshel, K. M., Fremont, W. P., Bearden, C. E., & Kates, W. R. (2016). Atypical functional connectivity in resting-state networks of individuals with 22q11.2 deletion syndrome: associations with neurocognitive and psychiatric functioning. *J. Neurodev. Disord.*, *8*, 2. URL: http://www.jneurodevdisorders.com/content/8/1/2. doi:10.1186/s11689-016-9135-z.

McDonald-McGinn, D. M., Sullivan, K. E., Marino, B., Philip, N., Swillen, A., Vorstman, J. A. S., Zackai, E. H., Emanuel, B. S., Vermeesch, J. R., Morrow, B. E., Scambler, P. J., & Bassett, A. S. (2015). 22q11.2 deletion syndrome. *Nat. Rev. Dis. Prim.*, *1*, 15071. URL: http://dx.doi.org/10.1038/nrdp.2015.71http://10.0.4.14/nrdp.2015.71.

McIntosh, A. R., Kovacevic, N., & Itier, R. J. (2008). Increased brain signal variability accompanies lower behavioral variability in development. *PLoS Comput. Biol.*, *4*. doi:10.1371/journal.pcbi.1000106.

McIntosh, A. R., Kovacevic, N., Lippe, S., Garrett, D., Grady, C., & Jirsa, V. (2010). The development of a noisy brain. *Arch. Ital. Biol.*, *148*, 323–337. doi:10.4449/aib.v148i3.1225.

McIntosh, A. R., & Lobaugh, N. J. (2004). Partial least squares analysis of neuroimaging data: Applications and advances. *Neuroimage*, *23*, 250–263. doi:10.1016/j.neuroimage.2004.07.020.

Menon, V. (2011). Large-scale brain networks and psychopathology: A unifying triple network model. *Trends Cogn. Sci.*, *15*, 483–506. URL: http://dx.doi.org/10.1016/j.tics.2011.08.003. doi:10.1016/j.tics.2011.08.003.

Menon, V., & Uddin, L. Q. (2010). Saliency, switching, attention and control: a network model of insula function. *Brain Struct. Funct.*, (pp. 1–13). doi:10.1007/s00429-010-0262-0.

Miller, T. J., Mcglashan, T. H., Rosen, J. L., Cadenhead, K., Ventura, J., Mcfarlane, W., Perkins, D., Pearlson, G. D., & Woods, S. W. (1995). Prodromal Assessment With the Structured Interview for Prodromal Syndromes and the Scale of Prodromal Symptoms : Predictive Validity , Interrater Reliability , and Training to Reliability. *Schizophr. Bull.*, (pp. 703–716). URL: http://psycnet.apa.org/journals/szb/29/4/703/.

Misić, B., Mills, T., Taylor, M. J., & McIntosh, A. R. (2010). Brain noise is task dependent and region specific. *J. Neurophysiol.*, *104*, 2667–2676. doi:10.1152/jn.00648.2010.

Miskovic, V., Owens, M., Kuntzelman, K., & Gibb, B. E. (2016). Charting moment-to-moment brain signal variability from early to late childhood. *Cortex*, *83*, 51–61. doi:10.1016/j.cortex.2016.07.006.

Murphy, K., Jones, L., & Owen, M. (1999). High rates of schizophrenia in adults with velo-cardio-facial syndrome. *Arch. Gen. Psychiatry*, *56*, 940–945. URL: +http://dx.doi.org/10.1001/archpsyc.56.10.940. doi:10.1001/archpsyc.56.10.940.

Narr, K. L., Toga, A. W., Szeszko, P., Thompson, P. M., Woods, R. P., Robinson, D., Sevy, S., Wang, Y., Schrock, K., & Bilder, R. M. (2005). Cortical thinning in cingulate and occipital cortices in first episode schizophrenia. *Biol. Psychiatry*, *58*, 32–40. doi:10.1016/j.biopsych.2005.03.043.

Nekovarova, T., Fajnerova, I., Horacek, J., & Spaniel, F. (2014). Bridging disparate symptoms of schizophrenia: a triple network dysfunction theory. *Front. Behav. Neurosci.*, *8*, 171. URL: http://www.ncbi.nlm.nih.gov/pmc/articles/PMC4038855/pdf/fnbeh-08-00171.pdf. doi:10.3389/fnbeh.2014.00171.

Nomi, J. S., Bolt, T. S., Ezie, C., Uddin, L. Q., & Heller, A. S. (2017). Moment-to-moment BOLD Signal Variability Reflects Regional Changes in Neural Flexibility Across the Lifespan. *J. Neurosci.*, *37*, 3408–16. URL: http://www.jneurosci.org/lookup/doi/10.1523/JNEUROSCI.3408-16.2017. doi:10.1523/JNEUROSCI.3408-16.2017.

Oskarsdóttir, S., Vujic, M., & Fasth, A. (2004). Incidence and prevalence of the 22q11 deletion syndrome: a population-based study in Western Sweden. *Arch. Dis. Child.*, *89*, 148–151. doi:10.1136/adc.2003.026880.

Ottet, M.-C., Schaer, M., Cammoun, L., Schneider, M., Debbané, M., Thiran, J.-P., & Eliez, S. (2013). Reduced fronto-temporal and limbic connectivity in the 22q11.2 deletion syndrome: vulnerability markers for developing schizophrenia? *PLoS One*, *8*, e58429. URL: http://journals.plos.org/plosone/article?id=10.1371/journal.pone.0058429. doi:10.1371/journal.pone.0058429.

Padula, M., Schaer, M., Scariati, E., Maeder, J., Schneider, M., & Eliez, S. (2017). Multimodal investigation of triple network connectivity in patients with 22q11DS and association with executive functions. *Hum. Brain Mapp.*, *2189*, 2177–2189. doi:10.1002/hbm.23512.

Padula, M. C., Schaer, M., Scariati, E., Schneider, M., Van De Ville, D., Debbané, M., & Eliez, S. (2015). Structural and functional connectivity in the default mode network in 22q11.2 deletion syndrome. *J Neurodev Disord*, *7*, 23. URL: http://www.jneurodevdisorders.com/content/7/1/23. doi:10.1186/s11689-015-9120-y.

Pettersson-Yeo, W., Allen, P., Benetti, S., McGuire, P., & Mechelli, A. (2011). Dysconnectivity in schizophrenia: Where are we now? *Neurosci. Biobehav. Rev.*, *35*, 1110–1124. URL: http://dx.doi.org/10.1016/j.neubiorev.2010.11.004. doi:10.1016/j.neubiorev.2010.11.004.

Power, J. D., Barnes, K. a., Snyder, A. Z., Schlaggar, B. L., & Petersen, S. E. (2012). Spurious but systematic correlations in functional connectivity MRI networks arise from subject motion. *Neuroimage*, *59*, 2142–2154. URL: http://dx.doi.org/10.1016/j.neuroimage.2011.10.018. doi:10.1016/j.neuroimage.2011.10.018. arXiv:NIHMS150003.

Reich, W. (2000). Diagnostic Interview for Children and Adolescents (DICA). *J. Am. Acad. Child Adolesc. Psychiatry*, *39*, 59–66. URL: http://www.sciencedirect.com/science/article/pii/

S0890856709661013. doi:10.1097/00004583-200001000-00017.

Reid, M. A., Stoeckel, L. E., White, D. M., Avsar, K. B., Bolding, M. S., Akella, N. S., Knowlton, R. C., Den Hollander, J. A., & Lahti, A. C. (2010). Assessments of function and biochemistry of the anterior cingulate cortex in schizophrenia. *Biol. Psychiatry*, *68*, 625–633. URL: http://dx.doi.org/10.1016/j.biopsych.2010.04.013. doi:10.1016/j.biopsych.2010.04.013. arXiv:NIHMS150003.

Rihs, T. A., Tomescu, M. I., Britz, J., Rochas, V., Custo, A., Schneider, M., Debbané, M., Eliez, S., & Michel, C. M. (2013). Altered auditory processing in frontal and left temporal cortex in 22q11.2 deletion syndrome: A group at high genetic risk for schizophrenia. *Psychiatry Res. - Neuroimaging*, *212*, 141–149. doi:10.1016/j.pscychresns.2012.09.002.

Rogachov, A., Cheng, J. C., Erpelding, N., Hemington, K. S., Crawley, A. P., & Davis, K. D. (2016). Regional brain signal variability: a novel indicator of pain sensitivity and coping. *Pain*, *2*, 1. URL: http://content.wkhealth.com/linkback/openurl?sid=WKPTLP:landingpage{&}an=00006396-900000000-99466. doi:10.1097/j.pain.0000000000000665.

Sandini, C., Scariati, E., Padula, M. C., Schneider, M., Schaer, M., Van De Ville, D., & Eliez, S. (2017). Cortical dysconnectivity measured by structural covariance is associated with the presence of psychotic symptoms in 22q11.2 deletion syndrome. *Biol. Psychiatry Cogn. Neurosci. Neuroimaging*, . doi:10.1016/j.bpsc.2017.04.008.

Scariati, E., Padula, M. C., Schaer, M., & Eliez, S. (2016a). Long-range dysconnectivity in frontal and midline structures is associated to psychosis in 22q11.2 deletion syndrome. *J. Neural Transm.*, . URL: http://link.springer.com/10.1007/s00702-016-1548-z. doi:10.1007/s00702-016-1548-z.

Scariati, E., Schaer, M., Karahanoglu, I., Schneider, M., Richiardi, J., Debbané, M., Van De Ville, D., & Eliez, S. (2016b). Large-scale functional network reorganization in 22q11.2 deletion syndrome revealed by modularity analysis. *Cortex*, *2*. doi:10.1016/j.cortex.2016.06.004.

Scariati, E., Schaer, M., Richiardi, J., Schneider, M., Debbané, M., Van De Ville, D., & Eliez, S. (2014). Identifying 22q11.2 deletion syndrome and psychosis using resting-state connectivity patterns. *Brain Topogr*, *27*, 808–821. URL: http://link.springer.com/10.1007/s10548-014-0356-8. doi:10.1007/s10548-014-0356-8.

Schaer, M., Glaser, B., Ottet, M.-C., Schneider, M., Bach Cuadra, M., Debbané, M., Thiran, J.-P., & Eliez, S. (2010). Regional cortical volumes and congenital heart disease: a MRI study in 22q11.2 deletion syndrome. *J. Neurodev. Disord.*, *2*, 224–234. URL: http://link.springer.com/10.1007/s11689-010-9061-4. doi:10.1007/s11689-010-9061-4.

Schneider, M., Armando, M., Pontillo, M., Vicari, S., Debbané, M., Schultze-Lutter, F., & Eliez, S. (2016). Ultra high risk status and transition to psychosis in 22q11.2 deletion syndrome. *World Psychiatry*, *15*, 259–265. URL: http://www.ncbi.nlm.nih.gov/pubmed/27717277. doi:10.1002/wps.20347.

Schneider, M., Debbané, M., Lagioia, A., Salomon, R., D'Argembeau, A., & Eliez, S. (2012). Comparing the neural bases of self-referential processing in typically developing and 22q11.2 adolescents. *Dev. Cogn. Neurosci.*, *2*, 277–289. URL: http://dx.doi.org/10.1016/j.dcn.2011.12.004. doi:10.1016/j.dcn.2011.12.004.

Schneider, M., Schaer, M., Mutlu, A. K., Menghetti, S., Glaser, B., Debbané, M., & Eliez, S. (2014). Clinical and cognitive risk factors for psychotic symptoms in 22q11.2 deletion syndrome: A transversal and longitudinal approach. *Eur. Child Adolesc. Psychiatry*, *23*, 425–436. doi:10.1007/s00787-013-0469-8.

Schultze-Lutter, F., Michel, C., Schmidt, S. J., Schimmelmann, B. G., Maric, N. P., Salokangas, R. K., Riecher-Rössler, A., van der Gaag, M., Nordentoft, M., Raballo, A., Meneghelli, A., Marshall, M., Morrison, A., Ruhrmann, S., & Klosterkötter, J. (2015). EPA guidance on the early intervention in clinical high risk states of psychoses. *Eur. Psychiatry*, *30*, 405–416. doi:10.1016/j.eurpsy.2015.01.013.

Shenhav, A., Botvinick, M., & Cohen, J. (2013). The expected value of control: An integrative theory of anterior cingulate cortex function. *Neuron*, *79*, 217–240. URL: http://dx.doi.org/10.1016/j.neuron.2013.07.007. doi:10.1016/j.neuron.2013.07.007. arXiv:NIHMS150003.

Sridharan, D., Levitin, D. J., & Menon, V. (2008). A critical role for the right fronto-insular cortex in switching between central-executive and default-mode networks. *Proc Natl Acad Sci U S A*, *105*, 12569–12574. URL: http://www.ncbi.nlm.nih.gov/pubmed/18723676. doi:10.1073/pnas.0800005105. arXiv:arXiv:1408.1149.

Takahashi, T., Cho, R. Y., Mizuno, T., Kikuchi, M., Murata, T., Takahashi, K., & Wada, Y. (2010). Antipsychotics reverse abnormal EEG complexity in drug-naive schizophrenia: A multiscale entropy analysis. *Neuroimage*, *51*, 173–182. URL: http://dx.doi.org/10.1016/j.neuroimage.2010.02.009. doi:10.1016/j.neuroimage.2010.02.009.

Tan, G. M., Arnone, D., McIntosh, A. M., & Ebmeier, K. P. (2009). Meta-analysis of magnetic resonance imaging studies in chromosome 22q11.2 deletion syndrome (velocardiofacial syndrome). *Schizophr. Res.*, *115*, 173–181. URL: http://dx.doi.org/10.1016/j.schres.2009.09.010. doi:10.1016/j.schres.2009.09.010.

Tognoli, E., & Kelso, J. A. (2014). The Metastable Brain. *Neuron*, *81*, 35–48. URL: http://dx.doi.org/10.1016/j.neuron.2013.12.022. doi:10.1016/j.neuron.2013.12.022. arXiv:NIHMS150003.

Tomescu, M. I., Rihs, T. A., Becker, R., Britz, J., Custo, A., Grouiller, F., Schneider, M., Debbané, M., Eliez, S., & Michel, C. M. (2014). Deviant dynamics of EEG resting state pattern in 22q11.2 deletion syndrome adolescents: A vulnerability marker of schizophrenia? *Schizophr. Res.*, *157*, 175–181. URL: http://dx.doi.org/10.1016/j.schres.2014.05.036. doi:10.1016/j.schres.2014.05.036.

Tomescu, M. I., Rihs, T. A., Roinishvili, M., Karahanoglu, F. I., Schneider, M., Menghetti, S., Van De Ville, D., Brand, A., Chkonia, E., Eliez, S., Herzog, M. H., Michel, C. M., & Cappe, C. (2015). Schizophrenia patients and 22q11.2 deletion syndrome adolescents at risk express the same deviant patterns of resting state EEG microstates: A candidate endophenotype of schizophrenia. *Schizophr. Res. Cogn.*, *2*, 159–165. URL: http://dx.doi.org/10.1016/j.scog.2015.04.005. doi:10.1016/j.scog.2015.04.005.

Uddin, L. Q. (2015). Salience processing and insular cortical function and dysfunction. *Nat Rev Neurosci*, *16*, 55–61. URL: http://dx.doi.org/10.1038/nrn3857http://10.0.4.14/nrn3857.

Van Den Heuvel, M. P., & Fornito, A. (2014). Brain networks in schizophrenia. *Neuropsychol. Rev.*, *24*, 32–48. doi:10.1007/s11065-014-9248-7.

Wechsler, D. (1991). Weschler intelligence scale for children. *San Antonio, TX Psychol. Corp.*, .

Wechsler, D. (1997). Wechsler intelligence scale for adults. *London Psychol. Corp.*, .

Wu, C. W., Chen, C.-L., Liu, P.-Y., Chao, Y.-P., Biswal, B. B., & Lin, C.-P. (2011). Empirical Evaluations of Slice-Timing, Smoothing, and Normalization Effects in Seed-Based, Resting-State Functional Magnetic Resonance Imaging Analyses. *Brain Connect.*, *1*, 401–410. doi:10.1089/brain.2011.0018.

Yan (2010). DPARSF: a MATLAB toolbox for "pipeline" data analysis of resting-state fMRI. *Front. Syst. Neurosci.*, *4*, 1–7. doi:10.3389/fnsys.2010.00013.

Yu, R., Chien, Y. L., Wang, H. L. S., Liu, C. M., Liu, C. C., Hwang, T. J., Hsieh, M. H., Hwu, H. G., & Tseng, W. Y. I. (2014). Frequency-specific alternations in the amplitude of low-frequency fluctuations in schizophrenia. *Hum. Brain Mapp.*, *35*, 627–637. doi:10.1002/hbm.22203.

Zöller, D., Schaer, M., Scariati, E., Padula, M. C., Eliez, S., & Ville, D. V. D. (2017). Disentangling resting-state BOLD variability and PCC functional connectivity in 22q11.2 deletion syndrome. *Neuroimage*, *149*, 85–97. URL: http://dx.doi.org/10.1016/j.neuroimage.2017.01.064. doi:10.1016/j.neuroimage.2017.01.064.

Supplementary Materials

Table S1: Demographic characteristics of the five subjects with a psychotic disorder according to DSM-IV-TR criteria.

subject	diagnosis*	age	gender	FSIQ
S1	psychosis	24.97	female	63
S2	schizoaffective disorder	23.05	male	56
S3	psychosis	18.13	female	67
S4	schizophrenia	14.09	female	46
S5	psychosis	14.28	male	68

* The presence of psychiatric disorders was evalutated during a clinical interview with the patients using the Diagnostic Interview for Children and Adolescents Revised (DICA-R; Reich, 2000), the psychosis supplement from the Kiddie-Schedule for Affective Disorders and Schizophrenia Present and Lifetime version (K-SADS-PL; Kaufman et al., 1997) and the Structured Clinical Interview for DSM-IV Axis I Disorders (SCID-I; First et al., 1996)..

S1. Subjects already included in previous studies.

The cohort is partly overlapping with our previous resting-state fMRI studies: 30 subjects (8 PS+, 6 PS-, 16 HC) have been also included in Debbané et al. (2012), 51 subjects (10 PS+, 8 PS-, 33 HC) in Scariati et al. (2014), 56 subjects (10 PS+, 11 PS-, 35 HC) in Padula et al. (2015), 54 subjects (13 PS+, 9 PS-, 32 HC) in Scariati et al. (2016b), 79 subjects (16 PS+, 16 PS-, 47 HC) in Padula et al. (2017), 83 subjects (16 PS+, 19 PS-, 48 HC) in Zöller et al. (2017).

S2. Summary on subject exclusion criteria.

From our initial sample of 97 patients and 90 HCs between 10 and 30 years old, a total of 61 participants had to be excluded to ensure the good quality of the data. 4 subjects (3 with 22q11DS, 1 HC) were excluded because they reported having fallen asleep during the scanning session. Another 31 subjects (24 with 22q11DS, 7 HC) had to be excluded due to excessive motion of more than 3 mm in translation or 3° in rotation, and the data of 20 more subjects (7 with 22q11DS, 13 HC) were not used because parts of the cortex were not captured. From the remaining dataset, 6 patients with 22q11DS were excluded after motion scrubbing (Power et al. 2012, see paragraph *Preprocessing*) as less than 100 rs-fMRI scans, corresponding to 4 min of scanning time, remained after exclusion of frames with a framewise displacement below the threshold of 0.5 mm. Supplementary Table S2 shows a summary of motion data for the three groups.

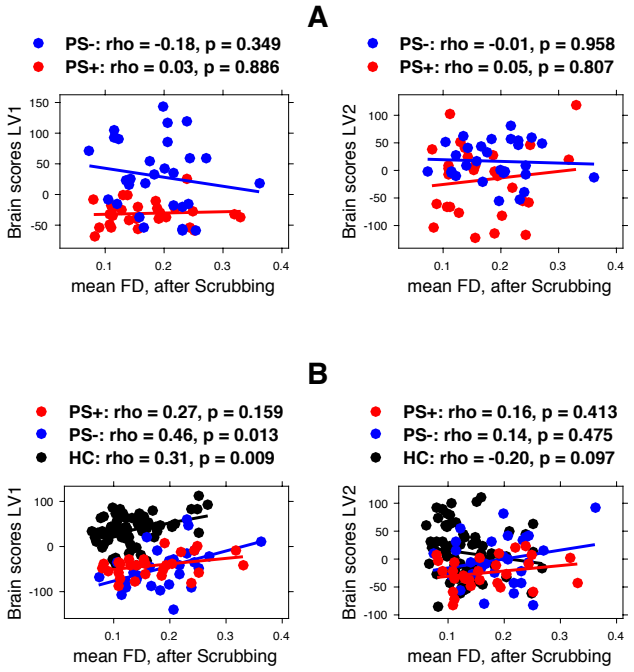

Figure S1: Correlation of brain scores with average framewise displacement (FD) for results comparing PS+ and PS- (A) and results comparing the two sub-groups with 22q11DS to healthy controls (B).

S3. Analysis of Motion effects.

In fMRI analysis, in particular when investigating the standard deviation of the BOLD signal, motion is a major concern. To explicitely test for motion effects in our data, we computed the correlation between brain scores and motion (i.e. the average framewise displacement). Figure S1 shows the correlations for the four correlation components.

Table S2: fMRI motion parameters. FD - framewise displacement.

		PS+	**PS-**	**HC**	**correlation with age (p value)**
Mean translation (mm)	x	0.15±0.18	0.17±0.16	0.13±0.14	0.0270 (0.7640)
	y	0.20±0.17	0.17±0.15	0.19±0.16	-0.1123 (0.2106)
	z	0.38±0.37	0.34±0.23	0.30±0.29	-0.1607 (0.0723)
Mean rotation (degree)	r_x	0.40±0.32	0.38±0.32	0.39±0.37	-0.0963 (0.2832)
	r_y	0.22±0.19	0.18±0.11	0.21±0.19	-0.0873 (0.3308)
	r_z	0.21±0.22	0.25±0.20	0.17±0.17	-0.1212 (0.1765)
Mean FD (mm), before scrubbing		0.21±0.12	0.25±0.12	0.16±0.09	-0.1711 (0.0555)
Mean FD (mm), after scrubbing		0.17±0.07	0.19±0.06	0.13±0.05	-0.1396 (0.1190)

Table S3: PS+ vs. PS- first correlation component: Table of clusters in brain salience pattern (see figure 2C).

Cluster	cluster size (voxels)	Max	AAL Regions (% of Cluster)
1	980	5.5996	Cingulum Mid L (40.00)
			Cingulum Mid R (27.24)
2	356	4.8309	Precuneus L (41.57)
			Parietal Inf L (27.25)
3	291	4.4196	Postcentral L (51.20)
4	260	4.1516	Postcentral L (61.15)
5	239	-4.7206	Temporal Inf R (61.51)
6	174	-4.9847	Frontal Mid Orb R (72.41)
7	162	4.1728	Insula R (58.64)
8	154	4.1949	Postcentral R (86.36)
9	145	4.5537	Frontal Sup R (46.90)
			Supp Motor Area R (32.41)
10	134	-3.8843	Parietal Inf R (46.27)
			Angular R (46.27)
11	133	3.7223	Parietal Sup R (66.92)
12	124	4.5115	Insula L (70.97)
13	123	-5.0961	Frontal Inf Oper R (48.78)
			Rolandic Oper R (36.59)
14	123	3.3118	Postcentral R (82.93)
15	121	-4.7685	Precentral L (48.76)
			Frontal Inf Oper L (33.06)
16	115	3.8668	Temporal Sup L (77.39)
17	105	4.0302	Caudate R (57.14)

Table S4: PS+ vs. PS- second correlation component: Table of clusters in brain salience pattern (see figure 3C).

Cluster	cluster size (voxels)	Max	AAL Regions (% of Cluster)
1	2390	5.6646	Occipital Mid L (24.98)
			Occipital Sup R (14.94)
			Occipital Mid R (12.89)
2	629	-4.9480	Frontal Mid L (34.02)
			Frontal Inf Tri L (17.17)
3	283	-5.4507	Frontal Sup L (37.46)
			Supp Motor Area L (31.80)
4	118	3.7825	Parietal Inf L (68.64)
5	114	-4.9117	Supp Motor Area R (57.89)
6	112	-4.3542	Temporal Sup R (100.00)
7	102	-6.3650	Supp Motor Area R (66.67)
8	98	4.2737	Fusiform L (69.39)

Table S5: 22q11DS vs. HC first correlation component: Table of clusters in brain salience pattern (see figure 4C).

Cluster	cluster size (voxels)	Max	AAL Regions (% of Cluster)
1	2944	-8.4020	Temporal Inf L (21.81)
			Temporal Mid L (15.05)
			Temporal Pole Sup L (11.55)
			Insula L (9.78)
2	1855	-10.9609	Temporal Sup R (15.36)
			Temporal Pole Sup R (13.42)
			Caudate R (12.78)
			Insula R (11.70)
3	1616	7.3895	Precuneus R (20.05)
			Calcarine L (19.25)
			Calcarine R (17.57)
4	1141	5.4858	Frontal Mid R (40.14)
			Frontal Mid Orb R (28.66)
5	951	-5.3670	Paracentral Lobule L (22.92)
			Precuneus L (19.03)
			Supp Motor Area L (15.98)
6	854	6.6592	Parietal Inf R (43.33)
			Temporal Mid R (25.29)
7	688	6.5589	Parietal Inf L (69.04)
8	499	-4.5475	Temporal Inf R (45.49)
			Hippocampus R (22.85)
9	403	-4.6535	Occipital Mid L (45.66)
			Occipital Inf L (30.52)
10	379	5.8835	Frontal Mid Orb L (51.45)
11	304	4.5216	Frontal Sup Medial L (50.99)
12	293	4.5203	Precentral L (54.61)
13	284	-5.4070	Thalamus L (96.83)
14	283	7.7556	Cingulum Mid R (34.28)
			Cingulum Post L (22.61)
15	275	-5.7140	Supp Motor Area R (70.18)
16	258	4.9003	Frontal Mid R (46.51)
			Frontal Inf Oper R (29.46)
17	250	5.7538	Thalamus R (95.20)
18	235	4.6995	Occipital Mid R (59.15)
19	201	4.6118	Cingulum Ant R (37.81)
			Frontal Sup Orb Medial L (26.37)
20	139	-3.8166	Postcentral R (58.27)
21	131	-5.2702	Occipital Sup L (53.44)
22	127	4.8752	Frontal Mid L (54.33)
23	118	4.5912	Temporal Mid L (100.00)
24	111	4.1011	Frontal Mid L (59.46)
25	110	3.6418	Occipital Mid L (69.09)
26	108	-4.1782	Putamen R (100.00)
27	106	-4.7828	Occipital Sup R (66.04)

Table S6: 22q11DS vs. HC second correlation component: Table of clusters in brain salience pattern (see figure 5C).

Cluster	cluster size (voxels)	Max	AAL Regions (% of Cluster)
1	3048	5.9324	Frontal Mid L (18.18)
			Supp Motor Area L (13.32)
			Supp Motor Area R (11.88)
			Frontal Sup L (10.66)
2	408	4.0058	Parietal Inf L (67.16)
3	380	-4.6755	Temporal Inf R (58.95)
4	347	-5.0529	Caudate L (17.58)
			Frontal Sup Orb L (15.27)
			Rectus L (14.41)
			Rectus R (12.39)
5	226	4.3457	Temporal Sup R (61.95)
6	218	-3.8788	Occipital Mid R (54.13)
7	207	-5.3421	Fusiform L (43.48)
			ParaHippocampal L (31.88)
8	199	-4.7324	Temporal Inf L (79.40)
9	199	-4.3567	Frontal Inf Oper L (33.17)
			Precentral L (29.65)
10	123	-4.9940	Frontal Inf Oper R (35.77)
			Rolandic Oper R (33.33)
11	123	-4.7006	Frontal Mid L (93.50)
12	119	-5.0014	Putamen R (70.59)
13	115	-5.0571	Fusiform R (52.17)
14	114	-3.9913	Cuneus L (52.63)
15	102	-3.9348	Occipital Mid L (100.00)
16	101	-3.8270	Amygdala R (53.47)
17	97	3.6622	Postcentral R (64.95)